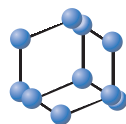


## RESEARCH ARTICLE

BENTHAM  
SCIENCE

## Synthesis of New Cyclic Imides Derived from Safrole, Structure- and Ligand-based Approaches to Evaluate Potential New Multitarget Agents Against Species of Leishmania



José A. de Sousa Luis<sup>1,4,\*</sup>, Normando A. da Silva Costa<sup>2</sup>, Cristiane C.S. Luis<sup>3</sup>, Bruno F. Lira<sup>2</sup>, Petrónio F. Athayde-Filho<sup>2</sup>, Tatjana K. de Souza Lima<sup>4</sup>, Juliana da Câmara Rocha<sup>4</sup>, Luciana Scotti<sup>4</sup> and Marcus T. Scotti<sup>4,\*</sup>

<sup>1</sup>Education and Health Center, Federal University of Campina Grande, Cuité, Paraíba, Brazil; <sup>2</sup>Research Laboratory on Biofuels and Organic Synthesis, Chemistry Department, Federal University of Paraíba, João Pessoa, Paraíba, Brazil; <sup>3</sup>Postgraduate Program in Nutrition Sciences, Federal University of Paraíba, João Pessoa, Paraíba, Brazil; <sup>4</sup>Postgraduate Program in Natural Products and Synthetic Bioactive, Federal University of Paraíba, João Pessoa, Paraíba, Brazil

**Abstract: Background:** Leishmaniasis is a neglected disease that does not have adequate treatment. It affects around 12 million people around the world and is classified as a neglected disease by the World Health Organization. In this context, strategies to obtain new, more active and less toxic drugs should be stimulated. Sources of natural products combined with synthetic and chemoinformatic methodologies are strategies used to obtain molecules that are most likely to be effective against a specific disease. Computer-Aided Drug Design has become an indispensable tool in the pharmaceutical industry and academia in recent years and has been employed during various stages of the drug design process.

**Objectives:** Perform structure- and ligand-based approaches, synthesize and characterize some compounds with materials available in our laboratories to verify the method's efficiency.

**Methods:** We created a database with 33 cyclic imides and evaluated their potential anti-Leishmanial activity (*L. amazonensis* and *L. donovani*) through ligand- and structure-based virtual screening. A diverse set selected from ChEMBL databanks of 818 structures (*L. donovani*) and 722 structures (*L. amazonensis*), with tested anti-Leishmanial activity against promastigotes forms, were classified according to  $pIC_{50}$  values to generate and validate a Random Forest model that shows higher statistical indices values. The structures of four different *L. donovani* enzymes were downloaded from the Protein Data Bank and the imides' structures were submitted to molecular docking. So, with available materials and technical feasibility of our laboratories, we have synthesized and characterized seven compounds through cyclization reactions between isosafrole and maleic anhydride followed by treatment with different amines to obtain new cyclic imides to evaluate their anti-Leishmanial activity.

**Results:** *In silico* study allowed us to suggest that the cyclic imides **5**<sub>16, 25, 31, 24, 32, 2, 3, 22</sub> can be tested as potential multitarget molecules for leishmanial treatment, presenting activity probability against four strategic enzymes (Topoisomerase I, *N*-myristoyltransferase, cyclophilin and *O*-acetylserine sulfhydrylase). The compounds synthesized and tested presented  $pIC_{50}$  values less than 4.7 for *Leishmania amazonensis*.

**Conclusion:** After combined approach evaluation, we have synthesized and characterized seven cyclic imides by IR, <sup>1</sup>H NMR, <sup>13</sup>C-APT NMR, COSY, HETCOR and HMBC. The compounds tested against promastigote forms of *L. amazonensis* presented  $pIC_{50}$  values less than 4.7, showing that our method was efficient in predicting true negative molecules.

**Keywords:** Cyclic imides, safrole, virtual screening, molecular docking, *Leishmania amazonensis*, *Leishmania donovani*, anti-leishmania activity.

\*Address correspondence to these authors at the Postgraduate Program in Natural Products and Synthetic Bioactive, Federal University of Paraíba, João Pessoa, Paraíba, Brazil; Tel: +55 83 99869-0415; E-mails: [mtscotti@gmail.com](mailto:mtscotti@gmail.com), [jalixluis@hotmail.com](mailto:jalixluis@hotmail.com)

### 1. INTRODUCTION

Despite the great development of modern medicinal chemistry, there are some microbial diseases that remain

without adequate chemotherapeutic agents, either due to problems of toxicity or resistance, among them is Leishmaniasis, which is a complex of infectious diseases caused by parasites of the family Trypanosomatidae and genus *Leishmania* [1, 2]. It affects around 12 million people around the world; there are reported cases in 98 countries spread across five continents, mainly in poor countries, causing the disease to be classified as a neglected disease by the World Health Organization [2-4]. It is the second most parasitic disease with the highest mortality and an estimated 350 million people are at risk of infection, being more prevalent in Brazil, Sudan, Ethiopia and India [5]. The protozoan *Leishmania* is transmitted to humans by insects of the genus *Phlebotomus* spp. and *Lutzomyia* spp. and diseases caused by infection are classified as Visceral Leishmaniasis and Cutaneous Leishmaniasis [6]. Another problem that has arisen recently is *Leishmania* coinfection in patients with Human Immunodeficiency Virus, mainly due to the development of resistance in the parasites to drugs commonly used in therapy (the pentavalent antimonial drugs Pentostan and Glucantime) [7].

In this context, strategies to obtain new, more active and less toxic drugs should be stimulated. Sources of natural products combined with synthetic and chemoinformatic methodologies are strategies used to obtain molecules that are most likely to be effective against a specific disease. Computer-Aided Drug Design has become an indispensable tool in the pharmaceutical industry and academia in recent years and has been employed during various stages of the drug design process. Initially, this method focuses on reducing the overall number of possible ligands; in the later stages, during lead optimization, the emphasis shifts to reducing experimental costs and the duration of time required to make a discovery [8-10].

Cyclic imides are a group of compounds with various biological activities that present a large class of compounds obtained by organic synthesis including several subclasses, among them maleimides, succinimides, glutarimides, phthalimides and naphthalimides, as well as their respective derivatives [11]. Because they are electronically neutral and of a hydrophobic nature, they easily cross cell membranes, leading to the important pharmacological effects of these imides, such as anti-inflammatory, antitumor, antimicrobial activities among others, which may be related to the size and characteristics of the groups present in the imidic ring, which may alter the steric characteristics of the molecules, altering their activity [12-16]. Another important class of substances for the pharmaceutical industry is the essential oils, which are natural products, which present as aromatic and oily liquids, evaporating easily when exposed to air at room temperature. Because of this, they are also known as volatile oils, other names are ethereal, refringent and essential oils. These oils are formed in several plants as byproducts of secondary metabolism [17]. These oils do not present as pure mixtures but rather mixtures with various proportions of different chemical structures such as acids, aldehydes, alcohols, ketones, esters, ethers, phenols, aromatic or terpene hydrocarbons [18]. As an example, we have sassafras oil (*Ocotea pretiosa*), which is rich in safrole, the precursor used in this study, because it has the methylenedioxy group that provides important characteristics to the derived molecules.

Taking into account the great medicinal importance of cyclic imides and their derivatives, as well as the excellent results found and published to date, the planning of 33 cyclic imides was carried out and a combined ligand- and structure-virtual chemical screening was carried out to select molecules with higher probability to show the desired effect against selected *Leishmania* targets. The selected compounds were synthesized and their anti-Leishmanial activities were evaluated.

## 2. MATERIAL AND METHODS

### 2.1. Dataset

We selected a diverse set of 818 structures from the ChEMBL database, (<https://www.ebi.ac.uk/chembl/>), which had been screened (*in vitro*) to inhibit the promastigote *L. donovani* and another diverse set of 722 structures which had been screened for promastigote form of *L. amazonensis*. The compounds were classified using values of  $-\log IC_{50}$  (mol/L) =  $pIC_{50}$ , which led us to assign 293 actives ( $pIC_{50} \geq 5.0$ ) and 525 inactives ( $pIC_{50} \leq 4.7$ ) for *L. donovani*; 253 actives ( $pIC_{50} \geq 5.0$ ) and 469 inactives ( $pIC_{50} \leq 4.7$ ) for *L. amazonensis*. We used a border in the  $pIC_{50}$  values looking for better prediction results. In this case,  $IC_{50}$  represented the concentration required for 50% inhibition of promastigote *L. donovani* and *L. amazonensis*. The compounds with  $pIC_{50}$  values between 4.7 and 5.0 were excluded to minimize the border effect and improve the discriminant power of the generated models. Our databank includes compounds 5<sub>1-33</sub>. For all structures, SMILES codes were used as input data to Marvin 17.18.0.1784, 2017, ChemAxon (<http://www.chemaxon.com>). We used Standardizer software [JChem 17.18.0.1784, 2017; ChemAxon (<http://www.chemaxon.com>)] to canonize structures, add hydrogens, perform aromatic form conversions, clean the molecular graph in three dimensions and save compounds in sdf format [9, 19].

### 2.2. Volsurf Descriptors

3-D structures were used as input data in the Volsurf+ program v. 1.0.7 and were subjected to molecular interaction fields (MIFs) to generate descriptors using the following probes: N1 (amide nitrogen-hydrogen bond donor probe), O (carbonyl oxygen-hydrogen bond acceptor probe), OH<sub>2</sub> (water probe) and DRY (hydrophobic probe) [20]. Additional non-MIF-derived descriptors were generated to create a total of 128 descriptors. Volsurf descriptors have been previously used to predict anti-Leishmanial activity of natural products on enzymes and predict the activity of some molecules [21, 22].

### 2.3. Models

KNIME 3.4.0 software (KNIME 3.4.0 the Konstanz Information Miner Copyright, 2003-2017), ([www.knime.org](http://www.knime.org)) [23] was used to perform all of the following analyses. The descriptors and class variables were imported from the Volsurf+ program, v. 1.0.7, and the data were divided using the "Partitioning" node with the "stratified sample" option to create a training set and a test set, encompassing 80% and 20% of the compounds, respectively. Although the compounds were selected randomly, the same proportion of ac-

tive and inactive samples was maintained in both sets. For internal validation, we employed cross-validation using 10 randomly selected, stratified groups, and the distributions according to activity class variables were found to be maintained in all validation groups and in the training set. Descriptors were selected, and a model was generated using the training set and the RF algorithm [24], using the WEKA nodes [25]. The parameters selected for RF included the following settings: number of trees to build = 1900, seed for random number generator = 1909501934341. The internal and external performances of the selected models were analyzed for sensitivity (true positive rate, *i.e.*, active rate), specificity (true negative rate, *i.e.*, inactive rate) and accuracy (overall predictability). In addition, the sensitivity and specificity of the ROC curve were found to describe the true performance with more clarity and accuracy. The plotted ROC curve shows the true positive (active) rate either versus the false positive rates or versus sensitivity (1: specificity). In a two-class classification, when a variable that is being investigated cannot be distinguished between the two groups (*i.e.*, when there is no difference between the two distributions), the area under the ROC curve equals 0.5, which is to say that the ROC curve will coincide with the diagonal. When there is a perfect separation of values between the two groups (*i.e.*, no overlapping of distributions), the area under the ROC curve equals 1, which is to say that the ROC curve will reach the upper left corner of the plot [26].

#### 2.4. Docking

The structure of *L. donovani* enzymes TOPI [27], NMT [28], Cyp [29] and OASS [30] downloaded from the Protein Data Bank (PDB) are summarized in Table 5 (<http://www.rcsb.org/pdb/home/home.do>). **5**<sub>1-33</sub> structures were submitted to molecular docking using the Molegro Virtual Docker, v. 6.0.1 (MVD). All of the water molecules were deleted from the enzyme structure, and the enzyme and compound structures were prepared using the same default parameter settings in the same software package. The docking procedure was performed using a GRID of 15 Å in radius and 0.30 Å in resolution to cover the ligand-binding site of the enzyme's structures. The Moldock score algorithm was used as the score function [31]. For all enzymes, the binding site was the same as the ligand present in the PDB file.

#### 2.5. Chemistry

Reagents used for the synthesis: maleic anhydride (Merck, 99%), potassium hydroxide (Vetec, 85%), phenylamine (Aldrich, 99.5%), benzylamine (Riedel, 99%), 4-aminobenzoic acid (Vetec, 99%), sulfanilamide (Vetec, 99%), 4-chloro-3-nitroaniline (Richem, 98%), 4-bromo-3-nitroaniline (Richem, 99%), 4-fluoro-3-nitroaniline (Richem, 99%) and safrole (Aldrich, 97%). Solvents used for the synthesis of the compounds: water, chloroform (Merck), deuterated chloroform (Isotec), DMSO (Vetec), ethanol (Merck), methanol (Merck), acetic acid (Merck), *n*-butanol, dichloromethane and toluene (Vetec). Infrared spectra were recorded on a BOMEM spectrometer MB100 model M Series (LA-SOM - CCEN - UFPB) on KBr pellets. Absorption bands are expressed in cm<sup>-1</sup>, in the range of 4000-400 cm<sup>-1</sup>. 1-D and 2-D <sup>1</sup>H and <sup>13</sup>C NMR spectra were obtained on a VARIAN

MERCURY apparatus at 60, 200 and 500 MHz for <sup>1</sup>H and 15, 50 and 125 MHz for <sup>13</sup>C (Analytical Center-CBIOTEC-UFPB), using tetramethylsilane (TMS) as the internal reference and the solvents dimethyl sulfoxide (DMSO-*d*<sub>6</sub>) and chloroform (CDCl<sub>3</sub>) to solubilize the samples. The chemical shifts ( $\delta$ ) were measured in units of parts per million (ppm) and the coupling constants in hertz (Hz). The melting points were determined on a heating plate MQAPF-3 (LPBS-DQ/UFPB) and were not corrected.

##### 2.5.1. Preparation of Isosafrole (6,7-methylenedioxypropenylbenzene) (2)

10 g (62 mmol, 9.1 mL) of safrole (**1**) and 50 mL (150 mmol) of a 3 M solution of KOH in *n*-butanol were added to a 125 mL flask equipped with reflux condenser and magnetic stirrer. The reaction was kept under stirring at reflux for 6 h. After this time, the mixture was neutralized with 10% HCl and the organic phase was washed successively with distilled water and aqueous NaCl solution to provide 9.5 g (8.65 mL, 95%) of isosafrole (**2**) as a colorless liquid. <sup>1</sup>H NMR, (60 MHz, DMSO-*d*<sub>6</sub>,  $\delta$ ): 1.82 (d, 3H), 5.82 (s, 2H), 6.73-6.92 (m, 5H). <sup>13</sup>C NMR, (15 MHz, DMSO-*d*<sub>6</sub>,  $\delta$ ): 148.2, 146.8, 132.2, 130.5, 123.3, 120.2, 108.0, 105.4, 100.9, 18.1.

##### 2.5.2. Preparation of 11,12-methylenedioxy-5-methyl-3,4,5,6-tetrahydronaphthalene-2,15-dicarboxylic Anhydride (4)

A mixture containing isosafrole (**2**) (13 g, 80 mmol), maleic anhydride (**3**) (10 g, 101 mmol - excess) and xylene (40 mL) was refluxed for about 3 h at a temperature of about 100 °C. After reflux the reaction mixture was cooled and precipitated, the solid obtained was washed with ethanol and extracted with hot chloroform to afford 9.36 g of (**4**) as pale-yellow crystals. Yield: 46%. Mp: 141°C - literature 142-143°C [32]. IR (KBr,  $\nu$  cm<sup>-1</sup>): 2978, 2935, 2902 (C-H) 1788, 1726 (C=O); 1502, 1483 (C=C); 1388 (CH); 1236, 1033 (C-O); 910, 866, 756 (aromatic). <sup>1</sup>H NMR, (60 MHz, DMSO-*d*<sub>6</sub>,  $\delta$ ): 1.06 (s, 1H); 2.59 (m, 3H); 3.68 (dd, 3H); 4.46 (d, 1H); 5.96 (t, 2H); 6.68 (s, 1H); 6.97 (s, 1H).

##### 2.5.3. General Procedure for the Preparation of the Cyclic Imides

The substituted aniline (1.5 mmol) and (**4**) (1.5 mmol) in 3.0 mL acetic acid (or amount needed to solubilize the solids well) were dissolved in a flask, the reaction mixture was refluxed for about 3 h after cooling the solution, the reaction mixture was allowed to stand until precipitation, filtered and washed with distilled water and the solid obtained was recrystallized from ethanol.

##### 2.5.3.1. Preparation of 1-(19-fluoro-18-nitrophenyl)-11,12-methylenedioxy-5-methyl-3,4,5,6-tetrahydronaphthalene-2,15-dicarboxyimide (5<sub>1</sub>)

Compound **5**<sub>1</sub> was obtained as pale-yellow crystals. Yield: 70%. Mp: 180-182 °C. IR (KBr,  $\nu$ , cm<sup>-1</sup>) 3082 (C-H, aromatic); 2962, 2920, 2877 (C-H, aliphatic); 1707 (C=O) 1502, 1483 (C=C), aromatic). <sup>1</sup>H NMR (200 MHz, DMSO-*d*<sub>6</sub>,  $\delta$ ) 3.52 (dd, *J* = 8.9, 5.7 Hz, 1H); 4.27 (d, *J* = 9.0 Hz, 1H); 2.26 (m, 1H), 2.61 (m, 2H); 6.74 (s, 1H); 7.09 (s, 1H); 5.98 (d, *J* = 15.8 Hz, 2H); 1.13 (d, *J* = 7.2 Hz, 3H); 8.17 (d, *J* = 2.0 Hz, 1H); 7.78-7.70 (m, 1H); 7.78 - 7.70 (m, 1H). <sup>13</sup>C

NMR (50 MHz, DMSO- $d_6$ ,  $\delta$ ) 176.5, 175.9, 153.9, 146.3, 145.7, 136.7, 135.0, 130.2, 128.6, 124.65, 122.1, 119.1, 109.3, 108.6, 100.8, 43.9, 43.4, 34.5, 29.9, 16.5.

**2.5.3.2. Preparation of 1-(19-bromo-18-nitrophenyl)-11,12-methylenedioxy-5-methyl-3,4,5,6-tetrahydronaphthalene-2,15-dicarboxyimide (5<sub>2</sub>)**

Compound **5<sub>2</sub>** was obtained as yellow crystals. Yield: 68%. Mp: 192-195 °C. IR (KBr,  $\nu$ ,  $\text{cm}^{-1}$ ) 3086 (C-H, aromatic); 2956, 2927, 2906, 2873 (C-H, aliphatic); 2852, 2821 (C-H, aliphatic); 1710 (C=O); 1541 (C=C, aromatic).  $^1\text{H}$  NMR (200 MHz, DMSO- $d_6$ ,  $\delta$ ) 3,50 (dd,  $J = 9.1, 5.5$  Hz, 1H); 4,25 (d, 1H); 2,22 (m, 1H); 2,45 (m, 2H); 6,72 (s, 1H); 7,06 (s, 1H); 5,96 (d,  $J = 18.8$  Hz, 2H), 1,11 (d,  $J = 7.0$  Hz, 3H); 8,05 (d,  $J = 7.3$  Hz, 1H); 8,03 (d,  $J = 7.3$ , 1H); 7,55 (dd,  $J = 8.6, 2.4$  Hz, 1H).  $^{13}\text{C}$  NMR (50 MHz, DMSO- $d_6$ ,  $\delta$ ) 176.4, 175.8, 149.6, 146.4, 145.8, 132.4, 132.2, 130.3, 124.0, 123.9, 122.1, 112.9, 109.3, 108.7, 100.9, 43.9, 43.5, 34.6, 29.9, 16.7.

**2.5.3.3. Preparation of 1-(19-chloro-18-nitrophenyl)-11,12-methylenedioxy-5-methyl-3,4,5,6-tetrahydronaphthalene-2,15-dicarboxyimide (5<sub>3</sub>)**

Compound **5<sub>3</sub>** was obtained as pale-yellow crystals. Yield: 72.8%. Mp: 198-200 °C. IR (KBr,  $\nu$ ,  $\text{cm}^{-1}$ ) 2958, 2929, 2910 (C-H, aliphatic); 1708 (C=O); 1541, 1479 (C=C, anel aromatic); 1388 ( $\text{CH}_3$ ).  $^1\text{H}$  NMR (200 MHz, DMSO- $d_6$ ,  $\delta$ ) 3,52 (dd,  $J = 8.9, 5.7$  Hz, 1H); 4,28 (d,  $J = 8.9$  Hz, 1H); 2,25 (m, 1H); 2,60 (m, 2H) 6,75 (s, 1H); 7,08 (s, 1H); 5,98 (d,  $J = 17.8$  Hz, 2H); 1,08 (d,  $J = 7.0$  Hz, 3H); 8,12 (d,  $J = 2.4$  Hz, 1H); 7, 92 (d,  $J = 8.7$  Hz, 1H); 7, 68 (dd,  $J = 8.7, 2.4$  Hz, 1H).  $^{13}\text{C}$  NMR (50 MHz, DMSO- $d_6$ ,  $\delta$ ) 176.4, 175.8, 147.5, 146.4, 145.8, 132.4, 131.9, 130.3, 124.8, 124.2, 124.0, 122.1, 109.3, 108.7, 100.9, 43.9, 43.5, 34.6, 29.9, 16.7.

**2.5.3.4. Preparation of para-(11,12-methylenedioxy-5-methyl-3,4,5,6-tetrahydronaphthalene-2,15-icarboxyimide)-benzoic Acid (5<sub>4</sub>)**

Compound **5<sub>4</sub>** was obtained as brown crystals. Yield: 72.5%. Mp: 214 °C. IR (KBr,  $\nu$ ,  $\text{cm}^{-1}$ ) 3458 (OH); 2964, 2924, 2902 (C-H, aliphatic); 1708 (C=O); 1382 ( $\text{CH}_3$ ).  $^1\text{H}$  NMR (200 MHz, DMSO- $d_6$ ,  $\delta$ ) 3,56 (dd,  $J = 8.8, 5.6$  Hz, 1H); 4,27 (d,  $J = 8.8$  Hz, 1H); 2,27 (m, 1H); 2,57 (m, 2H); 6,74 (s, 1H); 7,08 (s, 1H); 5,98 (d,  $J = 15.6$  Hz, 2H); 1,06 (d,  $J = 7.0$  Hz, 3H); 7,39 (d,  $J = 8.4$  Hz, 1H); 8,03 (d,  $J = 8.4$  Hz, 1H); 8,03 (d,  $J = 8.4$  Hz, 1H); 7,39 (d,  $J = 8.4$  Hz, 1H).  $^{13}\text{C}$  NMR (50 MHz, DMSO- $d_6$ ,  $\delta$ ) 176.2, 176.1, 166.6, 146.3, 145.7, 136.0, 130.1, 129.9, 129.9, 129.8, 127.0, 127.0, 122.2, 109.3, 108.7, 100.7, 43.9, 43.2, 34.6, 29.7, 16.3.

**2.5.3.5. Preparation of 1-(11,12-methylenedioxy-5-methyl-3,4,5,6-tetrahydronaphthalene-2,15-dicarboxyimide)-p-benzenesulfonylamine (5<sub>5</sub>)**

Compound **5<sub>5</sub>** was obtained as pale-yellow crystals. Yield: 75%. Mp: 280 °C. IR (KBr,  $\nu$ ,  $\text{cm}^{-1}$ ) 3387, 3240 (N-H); 3105 (C-H, aromatic); 2974, 2916 (C-H, aliphatic); 1695 (C=O); 1595 ( $\text{NH}_2$ ); 1500, 1485 (C=C, aromatic), 1394 (CH), 1336, 1035 (S=O); 1035 (S=O).  $^1\text{H}$  NMR (200 MHz, DMSO- $d_6$ ,  $\delta$ ) 3.52 (dd,  $J = 8.8, 5.8$  Hz, 1H), 4,29 (d,  $J = 8.9$  Hz, 1H); 2,28 (m, 1H); 2,61 (m, 2H); 6,77 (s, 1H); 7,10 (s, 1H); 5,98 (d,  $J = 7.7$  Hz, 2H); 1,09 (d,  $J = 6.8$  Hz 3H); 8, 93

(d,  $J = 8.6$  Hz, 1H); 7,47 (d,  $J = 8.6$  Hz, 1H); 7,47 (d,  $J = 8.6$  Hz, 1H); 8,93 (d,  $J = 8.6$  Hz, 1H); 7,48 (s, 2H -  $\text{NH}_2$ ).  $^{13}\text{C}$  NMR (50 MHz, DMSO- $d_6$ ,  $\delta$ ) 176.9, 176.2, 146.4, 145.8, 143.9, 135.1, 129.9, 127.7, 127.7, 126.6, 126.6, 122.3, 109.3, 108.8, 100.9, 43.9, 43.3, 34.7, 29.8, 16.4.

**2.5.3.6. Preparation of 1-benzyl-11,12-methylenedioxy-5-methyl-3,4,5,6-tetrahydronaphthalene-2,15-dicarboxyimide (5<sub>6</sub>)**

Compound **5<sub>6</sub>** was obtained as pale-yellow crystals. Yield: 82.7%. Mp: 139-140 °C. IR (KBr,  $\nu$ ,  $\text{cm}^{-1}$ ) 2966, 2912 (C-H, aliphatic); 1693 (C-O); 1504, 1485 (C=C, aromatic); 1398 ( $\text{CH}_3$ ).  $^1\text{H}$  NMR (200 MHz, DMSO- $d_6$ ,  $\delta$ ) 3,36 (dd,  $J = 8.9, 5.8$  Hz, 1H); 4,14 (d,  $J = 8.7$  Hz, 1H); 2,23 (m, 1H); 2,52 (m, 2H); 6,70 (s, 1H) 7,07 (s, 1H); 5,97 (d,  $J = 7.3$  Hz, 2H); 0,96 (d,  $J = 6.3$  Hz, 3H); 7,23 (m, 5H); 4,55 (s, 2H).  $^{13}\text{C}$  NMR (50 MHz, DMSO- $d_6$ ,  $\delta$ ) 177.7, 177.1, 146.2, 145.7, 136.2, 129.9, 128.6, 128.6, 128.4, 127.5, 127.4, 122.6, 109.2, 108.6, 100.9, 46.6, 43.2, 41.5, 34.6, 29.9, 16.5.

**2.5.3.7. Preparation of 1-phenyl-11,12-methylenedioxy-5-methyl-3,4,5,6-tetrahydronaphthalene-2,15-dicarboxyimide (5<sub>7</sub>)**

Compound **5<sub>7</sub>** was obtained as pale-yellow crystals. Yield: 82%. Mp: 246-248 °C-literature 249 °C. IR (KBr,  $\nu$ ,  $\text{cm}^{-1}$ ) 3093 (C-H, aromatic); 2922, 2982, 2841 (C-H, aliphatic); 1681 (C=O); 1591, 1573 (C=C, aromatic); 1424 ( $\text{CH}_3$ ); 1321, 1091 (C-O).  $^1\text{H}$  NMR (200 MHz, DMSO- $d_6$ ,  $\delta$ ) 3,49 (d,  $J = 8.9$  Hz, 1H); 4,25 (d,  $J = 8.9$  Hz 1H); 2,29 (m, 1H); 2,61 (m, 2H); 5,99 (d,  $J = 9.7$  Hz, 2H); 6,75 (s, 1H); 7,10 (s, 1H); 7,48 (t,  $J = 7.8$  Hz, 2H); 7,22 (dd,  $J = 8.9, 1.5$  Hz, 2H); 7,41 (t,  $J = 7.9$  Hz, 1H); 7,22 (dd,  $J = 8.9, 1.5$  Hz, 2H).  $^{13}\text{C}$  NMR (50 MHz, DMSO- $d_6$ ,  $\delta$ ) 177.0, 176.4, 146.3, 145.7, 132.3, 129.7, 128.9, 128.9, 128.4, 127.0, 127.0, 122.4, 109.3, 108.7, 100.8, 43.8, 43.0, 34.7, 29.7, 16.3.

## 2.6. Biological Activity

The parasite *Leishmania* (*Leishmania*) *amazonensis* (IFLA/BR/1967/PH8) in promastigote form was cultivated in Schneider's medium (Sigma-Aldrich, St. Louis, MO, USA) supplemented with 20% bovine fetal serum, 1% male human urine and antibiotics (penicillin 200 U/mL and streptomycin 0.1 mg/mL) (Gibco, CA) kept incubated in a biological oxygen demand (B.O.D.) incubator at 26°C. The colorimetric assay agent MTT (3-(4,5-dimethylthiazol-2-yl)-2,5-diphenyltetrazolium bromide) is based on the dehydrogenase activity of cytosolic and mitochondrial enzymes that are able to reduce MTT (yellow coloration) and form a blue product, insoluble in water, a formazan salt. The MTT assay was used to evaluate the anti-*Leishmania* activity of compounds **5<sub>1-7</sub>**, with determination of cell viability by calculating the  $IC_{50}$ . In a 96-well plate was added 100  $\mu\text{L}$  supplemented Schneider medium and about  $1 \times 10^6$  promastigotes/well of *L. amazonensis*. Subsequently, they were added to triplicate test substances previously diluted in supplemented Schneider medium to a final volume of 100  $\mu\text{L}$  in each well at concentrations of 100, 50, 25, 12.5, 6.25 and 3.125  $\mu\text{g/mL}$  of each compound previously diluted in half with Schneider DMSO. Then, the plate was incubated for 72 h in a B.O.D. oven at 26°C. At the end of incubation, 10  $\mu\text{L}$  of MTT diluted in PBS was added to a final concentration of 5 mg/mL. They

**Table 1.** Summary of training, internal cross-validation, test results and corresponding match results, which were obtained using the RF algorithm on the total set of 722 compounds tested against promastigotes forms of *L. amazonensis* (614 were in the training set and 108 in the test set).

-	Validation			Test		
	Samples	Match	% Match	Samples	Match	% Match
Active	253	215	70.23	38	25	65.79
Inactive	469	399	90.22	70	67	95.71
Overall	722	614	83.22	108	92	85.19

**Table 2.** Summary of training, internal cross-validation, test results and corresponding match results, which were obtained using the RF algorithm on the total set of 818 compounds tested against promastigotes forms of *L. donovani* (655 were in the training set and 163 in the test set).

-	Validation			Test		
	Samples	Match	% Match	Samples	Match	% Match
Active	293	235	71.06	58	46	79.31
Inactive	525	420	91.19	105	96	91.43
Overall	818	655	83.97	163	142	87.12

were incubated for another 4 h in a B.O.D. greenhouse at 26°C, and then 50 µL 10% sodium dodecylsulfate (Vetec<sup>®</sup>) was added. The plate was left overnight for dissolution of the formazan, and finally the absorbance of each well was read using a spectrophotometer (Spectramax Plus, Molecular Devices, Sunnyvale, CA, USA) at 570 nm. The negative control was performed in Schneider medium supplemented with 0.2% DMSO. The positive control was performed in the presence of amphotericin B as the reference drug. Assays were performed in triplicate and repeated three times on different days.

### 3. RESULTS AND DISCUSSIONS

#### 3.1. Computational Study

##### 3.1.1. Ligand-based VS Approach

The Volsurf (v 1.0.7) program generated 128 descriptors that, together with the dependent variables (binary classification) that described whether the compounds were active (A) or inactive (I), were used as input data in the KNIME program (v. 3.4.0) to generate the Random Forest (RF) model. For all compounds, the generation of all 128 descriptors by Volsurf+ was rapid, taking approximately 25 minutes using a computer with an i7 processor, running at 2.6 GHz, and equipped with 8 GB of RAM.

Table 1 summarizes the statistical indices of the RF model for the training, cross-validation and test sets for compounds tested against promastigotes forms of *L. amazonensis* and Table 2 for compounds tested against promastigotes forms of *L. donovani*. For the training set, the learning machine model gave the same hit rates for the inactive compounds and active compounds, which were 100%. However, for the cross-validation and test sets, the match rates

were better at predicting the inactive compounds in both studies (Tables 1 and 2); therefore, the specificity (true positive rate) was lower for the cross-validation and test sets (70.23% and 65.79%, respectively) than the sensitivity (true negative rate), which were 90.22% and 95.71%, respectively, in the model for *L. amazonensis* (Table 1). In the model for *L. donovani*, the specificities for the cross-validation and test sets were 71.06% and 79.31%, respectively, and the sensitivities were 91.19% and 91.43%, respectively (Table 2).

For both RF models, *L. amazonensis* and *L. donovani*, the ROC plot that was generated for the test set, which plotted the true positive (active) rate against the false positive rates had an area under the curve (AUC) value of approximately 0.88 and 0.91, respectively, which is significantly higher than 0.5 (Fig. 1). The Matthews Correlation Coefficient (MCC) values for cross-validation and test sets were 0.624 and 0.670, for the *L. amazonensis* RF model and 0.645 and 0.716 for the *L. donovani* RF model. Because an MCC value of 1 represents a perfect prediction, 0 represents random prediction, and -1 represents total disagreement between prediction and observation, the RF model shows significant MCC values.

Table 3 shows a prediction of activity, with their respective probabilities (p) calculated using the RF model for compounds **5**<sub>1-33</sub> against *L. amazonensis* and *L. donovani*. For values of  $p \geq 0.5$  the molecule was considered active (A);  $p < 0.5$  the molecule was considered inactive (I).

On the other hand, we evaluated the potential of synthesized imides as anti-Leishmanial leads against *L. donovani* using the RF model and docking on selected *Leishmania donovani* enzyme targets because only data deposited for this species were found in the Protein Data Bank (Tables 4, 5).

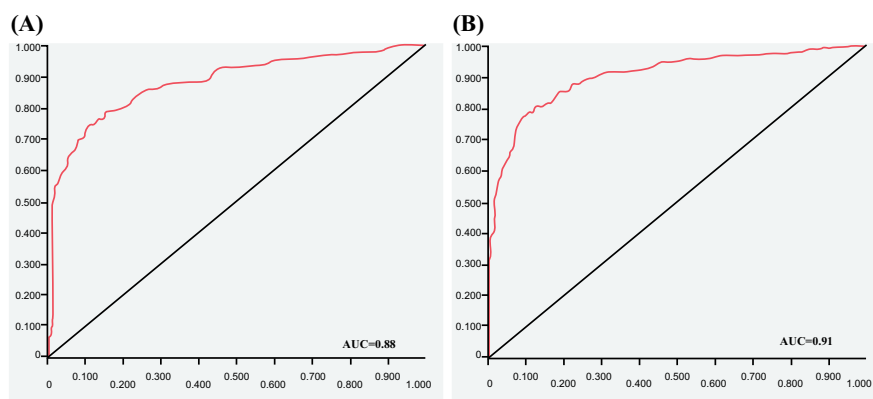


**Fig. (1).** ROCs plots generated by the selected RF models for the test set and values of the area under the curve (AUC). (a) For *L. amazonensis* and (b) for *L. donovani*. (A higher resolution / colour version of this figure is available in the electronic copy of the article).

**Table 3.** Prediction of activity, with their respective probabilities (*p*) calculated using the RF model for compounds 51-33 against *L. donovani* and *L. amazonensis*

Compound	<i>L. donovani</i>		<i>L. amazonensis</i>	
	Activity	<i>p</i>	Activity	<i>p</i>
5 <sub>1</sub>	A	0.78	I	0.39
5 <sub>2</sub>	A	0.81	I	0.47
5 <sub>3</sub>	A	0.81	I	0.43
5 <sub>4</sub>	I	0.37	I	0.26
5 <sub>5</sub>	I	0.37	I	0.32
5 <sub>6</sub>	A	0.51	I	0.37
5 <sub>7</sub>	A	0.75	I	0.35
5 <sub>8</sub>	A	0.62	I	0.28
5 <sub>9</sub>	A	0.58	I	0.32
5 <sub>10</sub>	A	0.51	A	0.59
5 <sub>11</sub>	A	0.52	I	0.30
5 <sub>12</sub>	A	0.59	I	0.30
5 <sub>13</sub>	A	0.54	I	0.40
5 <sub>14</sub>	A	0.66	I	0.29
5 <sub>15</sub>	A	0.69	I	0.35
5 <sub>16</sub>	A	0.82	I	0.43
5 <sub>17</sub>	I	0.39	I	0.29
5 <sub>18</sub>	A	0.61	I	0.39
5 <sub>19</sub>	I	0.47	I	0.37
5 <sub>20</sub>	A	0.51	I	0.31
5 <sub>21</sub>	I	0.46	I	0.30
5 <sub>22</sub>	A	0.68	A	0.51
5 <sub>23</sub>	I	0.48	I	0.31
5 <sub>24</sub>	A	0.71	A	0.56
5 <sub>25</sub>	A	0.75	A	0.61
5 <sub>26</sub>	I	0.39	I	0.25
5 <sub>27</sub>	A	0.66	I	0.39
5 <sub>28</sub>	A	0.64	I	0.45
5 <sub>29</sub>	A	0.65	I	0.36
5 <sub>30</sub>	A	0.63	A	0.63
5 <sub>31</sub>	A	0.71	A	0.62
5 <sub>32</sub>	A	0.53	A	0.62
5 <sub>33</sub>	A	0.53	A	0.64

**Table 4.** Data of the tested enzymes.

Enzyme	PDB ID	Resolution (Å)	Source	Ligand
TOPI	2B9S	2.27	<i>L. donovani</i>	VO <sub>4</sub>
NMT	5A27	1.42	<i>L. donovani</i>	2-oxopentadecyl-CoA
Cyp	3EOV	2.6	<i>L. donovani</i>	cyclosporin A
OASS	3T4P	1.79	<i>L. donovani</i>	Di(hydroxyethyl) ether

**Table 5.** Moldock score of best position of imides in enzyme targets.

ID	TOPI <sup>a</sup>	NMT <sup>b</sup>	Cyp <sup>c</sup>	OASS <sup>d</sup>
5 <sub>1</sub>	-98.89	-87.06	-77.36	-102.67
5 <sub>2</sub>	-103.97	-87.05	-77.43	-102.52
5 <sub>3</sub>	-103.79	-87.04	-77.43	-102.53
5 <sub>4</sub>	-115.74	-97.42	-72.70	-103.04
5 <sub>5</sub>	-109.16	-99.07	-72.40	-114.15
5 <sub>6</sub>	-104.11	-96.89	-70.99	-96.16
5 <sub>7</sub>	-107.26	-89.87	-70.80	-99.96

<sup>a</sup>Topoisomerase I; <sup>b</sup>*N*-myristoyltransferase; <sup>c</sup>cyclophilin; <sup>d</sup>*O*-acetylserine sulphydrylase.

**Table 6.** Activity of cyclic imides with the best performance in a docking study with each enzyme.  $p_c$  indicates the probability of activity from the Combined approach and Lipinski filters.

ID	Combined Probabilities ( $p_c$ )				Lipinski Filters <sup>*</sup>		
	TOPI <sup>a</sup>	NMT <sup>b</sup>	Cyp <sup>c</sup>	OASS <sup>d</sup>	clogP	DL	DS
5 <sub>16</sub>	0.60	0.62	0.68	0.63	3.71	-1.74	0.33
5 <sub>25</sub>	0.60	0.59	0.66	0.58	5.28	1.80	0.42
5 <sub>31</sub>	0.61	0.59	0.63	0.55	5.28	0.0	0.34
5 <sub>24</sub>	0.58	0.56	0.62	0.58	5.16	4.83	0.49
5 <sub>32</sub>	0.59	0.57	0.60	0.56	5.32	2.88	0.49
5 <sub>2</sub>	0.57	0.58	0.63	0.54	4.44	-7.23	0.21
5 <sub>3</sub>	0.55	0.55	0.60	0.50	4.32	-5.38	0.23
5 <sub>22</sub>	0.56	0.53	0.60	0.51	4.90	2.35	0.54

<sup>\*</sup> clogP (related to lipophilicity); DL (Drug-likeness); and DS (Drug-score). Values calculated using the OSIRIS Property Explorer program available at [www.organic-chemistry.org/prog/peo/](http://www.organic-chemistry.org/prog/peo/)

<sup>a</sup>Topoisomerase I; <sup>b</sup>*N*-myristoyltransferase; <sup>c</sup>cyclophilin; <sup>d</sup>*O*-acetylserine sulphydrylase.

A computational chemistry multitarget model to predict the results of experimental tests for Leishmania with significant success has been reported in the literature [33], so to finish the study, the combined probabilities of both Ligand approach and Structure approach were calculated by the formula:  $p_c = p_s + (1 + TN) \times p/2 + TN$ ; where  $p_c$  = Combined approach probability,  $p_s$  = Structure approach probability,  $p$  = Ligand approach probability, TN = True Negative probability and  $p_s = E_i/E_{\min}$  if  $E_i < E_{\text{ligand}}$ .

We used our *in silico* results of the cyclic imides to select structures that presented lower energy binding (eight compounds) from each enzyme (Table 5). After this step, looking for multitarget compounds, we selected imides with activity

against all enzymes, with probabilities above 50% (Table 6). The compounds 5<sub>16</sub>, 5<sub>25</sub>, 5<sub>31</sub>, 5<sub>24</sub>, 5<sub>32</sub>, 5<sub>2</sub>, 5<sub>3</sub> and 5<sub>22</sub> presents activity against the four enzymes. Analyzing the RF model (Table 4) it is possible to observe that the eight compounds were also classified as active by the model. Fig. (2) summarizes the virtual-screening methodology.

Fig. (3) shows hydrogen-bond interactions between cyclic imide 5<sub>16</sub>'s best position in Topoisomerase I (TOPI), *N*-myristoyltransferase (NMT), cyclophilin (Cyp) and *O*-acetylserine sulphydrylase (OASS). It is possible to observe that there is no pattern of interaction between the molecule and the active sites of the enzymes.

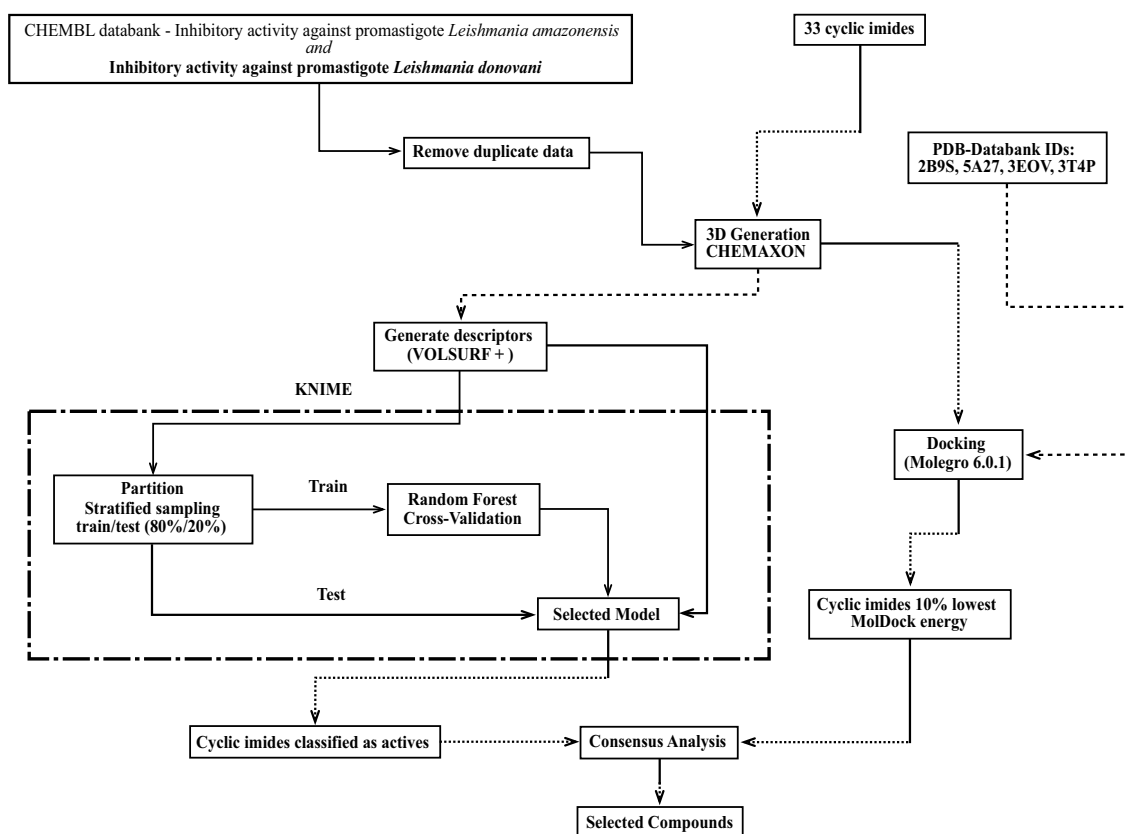
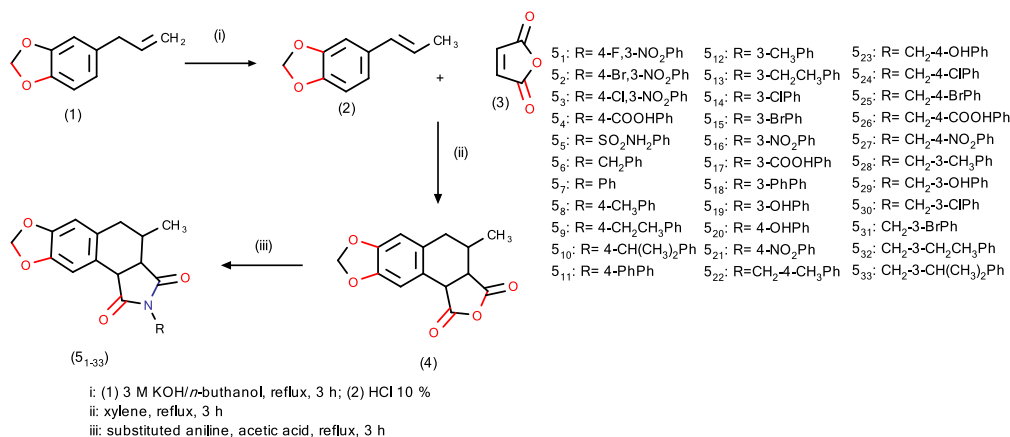


**Fig. (2).** Virtual-screening methodology used in this study. Solid black lines represent the set of 818 or 722 compounds used to generate the RF model and to validate it (solid gray line-external test set). Black round dotted lines represent the cyclic imides. Black dash-dot line represents both datasets (818 or 722 compounds and 33 cyclic imides). The black dash line represents the six enzyme structures from the PDB databank (2B9S, 5A27, 3EOV, 3T4P). The dash-dot border delimits the process performed in the KNIME software.



**Scheme 1.** The general synthetic procedure of the target compounds.

### 3.2. Chemistry

Seven molecules were synthesized. The first intermediate prepared was isosafrole. It was produced from safrole in a basic reaction medium through an isomerization. Reflux was used with KOH/*n*-butanol, which is a simple and cheap reaction and provides products with good yields [34]. The second step was the reaction of isosafrole with maleic anhydride using xylene as the solvent at 100 °C. This reaction is a cyclization (4 + 2), similar to a Diels-Alder reaction, the reaction cannot be considered purely Diels-Alder, which happens in a single phase and this undergoes an additional rear-

angement [32]. The final step is the reaction of 11,12-methylenedioxy-5-methyl-3,4,5,6-tetrahydronaphthalene-2,15-dicarboxylic anhydride (4) with different aromatic amines in acetic acid under reflux conditions. The mechanism of the reaction occurs simultaneously, starting with the attack of the nucleophile of the amino group to the carbonyl of the imidic ring because the carbon of the double bond is polarized, having partial positive charge. In this way, the nucleophile can enter, after which the ring ruptures through the exit of a molecule of H<sub>2</sub>O (favored by the high temperatures), forming the corresponding cyclic imides (Scheme 1).

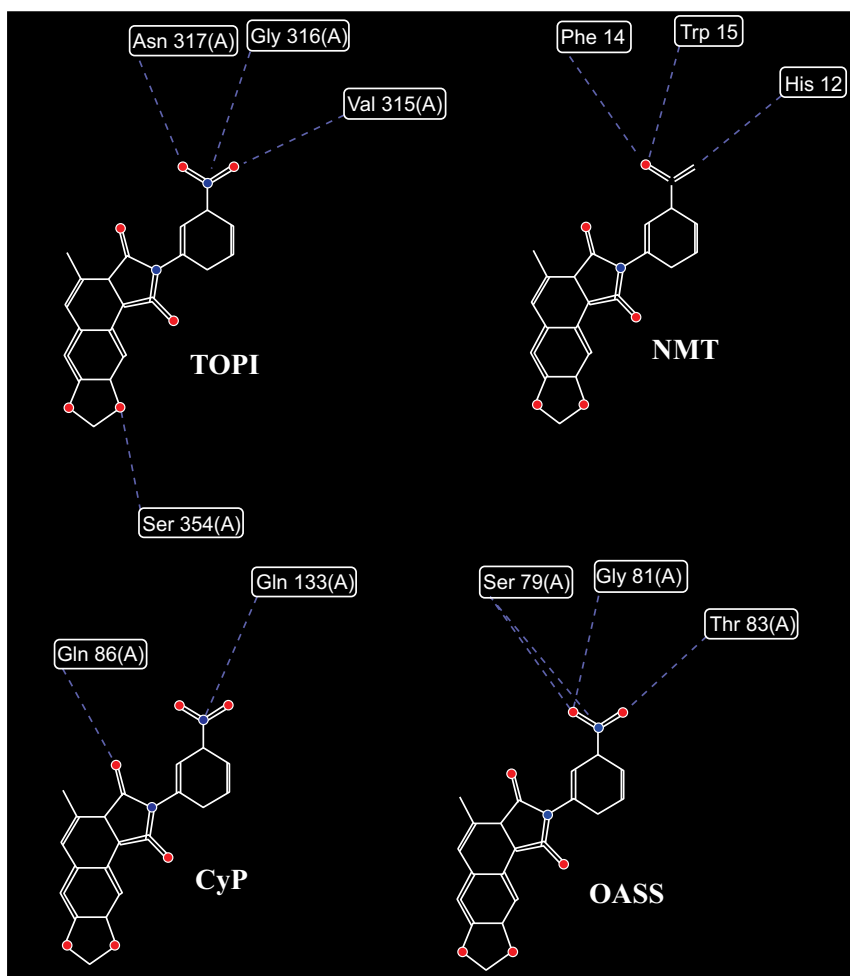


**Fig. (3).** Lowest-energy dock positions and energies of imide  $5_{16}$  with TOPI (-135.65), NMT (-110.06), CyP (-105.80) and OASS (-112.61). Dashed lines represent hydrogen-bond interactions. (A higher resolution / colour version of this figure is available in the electronic copy of the article).

### 3.2.1. Structural Characterization of Cyclic Imides

As a parameter for the characterization of cyclic imides, compound  $5_1$  was used as an example for the discussion of the main signals observed in the molecules under study. Assignments of the hydrogens and carbons performed for compound  $5_1$  were based on data obtained from five NMR experiments, namely,  $^1\text{H}$  NMR,  $^{13}\text{C}$ -APT NMR, COSY, HETCOR and HMBC. Table 7 summarizes the assignments made to each hydrogen and carbon of the molecule. The attributions of the hydrogens and carbons follow the numbering shown in Fig. (4). In the analysis of the  $^{13}\text{C}$ -APT NMR spectra at 50 MHz of  $5_1$ , the presence of 20 signals was observed, of which nine down signals were associated with hydrogenated carbons, one of which was assigned to trihydrogenated carbon at  $\delta$  16.54 ppm of (C-3), (C-4) and (C-5), and five of the aromatic carbons at  $\delta$  108.6, 109.3, 124.7, 119.1 and 135.0 ppm of carbons (C-9), (C-10), (C-17), (C-20) and (C-21), respectively. The remaining 11 signals, all up, two corresponded to aliphatic dihydrogenated carbons at  $\delta$  34.5 and 108.8 ppm of (C-6) and (C-13), respectively. Nine unhydrogenated carbons of the  $\text{sp}^2$  type, two of carbonyl carbons of (C-2) and (C-15) at  $\delta$  176.5 and 175.9 ppm respectively and seven quaternary carbons at  $\delta$  130.19, 122.1, 145.7, 146.3, 136.7, 128.6 and 153.3 ppm of the (C-

136.7, 128.6 and 153.3 ppm of the (C-7), (C-8), (C-11), (C-12), (C-16), (C-18) and (C-19) carbons, respectively.

The HETeronuclear CORrelation (HETCOR- $^1J_{\text{C-H}}$ ) two-dimensional (2-D) spectra analysis allowed correlating the  $^{13}\text{C}$  nuclei with the  $^1\text{H}$  directly attached to them (coupled) at  $\delta$  3.52 (H-3) with 43.9 (C-3);  $\delta$  4.27 (H-4) with 43.4 (C-4);  $\delta$  2.26 (H-5) with 29.9 (C-5);  $\delta$  2.61 (H-6) with 34.5 (C-6);  $\delta$  6.74 (H-9) with 108.6 (C-9);  $\delta$  7.09 (H-10) with 109.3 (C-10);  $\delta$  5.98 (H-13) with 100.8 (C-13);  $\delta$  1.13 (H-14) with 16.5 (C-14);  $\delta$  8.17 (H-17) with 124.7 (C-17);  $\delta$  7.78-7.70 (H-20) with 119.1 (C-20) and  $\delta$  7.78-7.70 (H-21) with 135.0 (C-21) ppm (Table 7).

Analysis of the 2-D spectroscopy (COSY- $^3J_{\text{H-H}}$  and  $^4J_{\text{H-H}}$ ) spectra allowed to correlate the  $^1\text{H}$  nuclei with  $^1\text{H}$  remote three and four bonds, respectively. We start our studies from the hydrogens of the methyl group, which is a good starting group. It appears as an intense doublet of hydrogens (H-14) at  $\delta$  1.13 ppm ( $J = 7.2$  Hz), which only couples with hydrogen (H-5) at  $\delta$  2.26 ppm. This coupling confirms that the  $\text{CH}_3$  group is terminal. The hydrogen of the (H-5) group at  $\delta$  2.26 ppm is also coupled with the hydrogen (H-6) at  $\delta$  2.61 ppm and (H-3) at  $\delta$  3.52 ppm, which, in turn, couples with the (H-4) at  $\delta$  4.27 ppm. Hydrogen (H-6) at  $\delta$  2.61 ppm

**Table 7.**  $^1\text{H}$  NMR (200 MHz) and  $^{13}\text{C}$  (50 MHz) data on (DMSO- $d_6$ ) of **5**<sub>1</sub> (Scheme 1). The atom labeled as 1 is nitrogen. The chemical shifts are ppm.

Carbon $\delta$ (ppm)	HETCOR/APT		COSY $\delta$ ( $^2J$ and $^3J_{\text{H-H}}$ ) <sup>c,e</sup>	HMBC $\delta$ ( $^2J$ and $^3J_{\text{C-H}}$ ) <sup>d</sup>
	$\delta$ ( $^{13}\text{C}$ ) <sup>a</sup>	$\delta$ ( $^1\text{H}$ ) <sup>b,e</sup>		
2	176.5	-	-	-
3	43.9	3.52 (dd, $J = 8.9, 5.7$ Hz, 1H)	4.27 (d, $J = 9.0$ Hz, H-4) and 2.26 (m, H-5)	16.5 (C-14); 29.9 (C-5); 176.5 (C-2) and 175.9 (C-15)
4	43.4	4.27 (d, $J = 9.0$ Hz, 1H)	3.52 (dd, $J = 8.9, 5.7$ Hz, 1H)	43.9 (C-3); 122.1 (C-8); 176.5 (C-2) and 175.9 (C-15)
5	29.9	2.26 (m, 1H)	3.52 (dd, $J = 8.9, 5.7$ Hz, H-3), 2.61 (m, H-6) and 1.13 (d, $J = 7.2$ Hz, H-14)	34.5 (C-6); 43.9 (C-3) and 16.5 (C-14)
6	34.5	2.61 (m, 2H)	2.26 (m, H-5)	43.9 (C-3); 29.9 (C-5); 108.6 (C-9) and 130.2 (C-7)
7	130.2	-	-	-
8	122.1	-	-	-
9	108.6	6.74 (s, 1H)	-	34.5 (C-6); 122.1 (C-8); 145.7 (C-11) and 146.3 (C-12)
10	109.3	7.09 (s, 1H)	-	43.4 (C-4); 130.2 (C-7); 145.7 (C-11) and 146.3 (C-12)
11	145.7	-	-	-
12	146.3	-	-	-
13	100.8	5.98 (d, $J = 15.8$ Hz, 2H)	-	145.7 (C-11) and 146.3 (C-12)
14	16.5	1.13 (d, $J = 7.2$ Hz, 3H)	2.26 (m, H-5)	43.9 (C-3) and 29.9 (C-5)
15	175.9	-	-	-
16	136.7	-	-	-
17	124.7	8.17 (d, $J = 2.0$ Hz, 1H)	7.78-7.70 (m, H-21)	153.9 (C-19) and 135.0 (C-21)
18	128.6	-	-	-
19	153.9	-	-	-
20	119.1	7.78-7.70 (m, 1H)	7.78-7.70 (m, H-21)	128.6 (C-18) and 135.0 (C-21)
21	135.0	7.78-7.70 (m, 1H)	7.78-7.70 (m, H-21) and 8.17 (d, $J = 2.0$ Hz, H-17)	124.7 (C-17) and 153.9 (C-19)

<sup>a</sup>Values deduced by  $^{13}\text{C}$ -APT NMR spectra; <sup>b</sup>Values obtained from 2-D heteronuclear correlations through one bond ( $^1J_{\text{C-H}}$ ) HETCOR; <sup>c</sup>Values obtained from 2-D homonuclear correlations through a ( $^2J_{\text{H-H}}$  and  $^4J_{\text{H-H}}$ ) COSY; <sup>d</sup>Values obtained from 2-D correlations through ( $^2J_{\text{C-H}}$ ) and ( $^3J_{\text{C-H}}$ ) HMBC. <sup>e</sup>Multiplicity of signals for  $^1\text{H}$  NMR: singlet (s); doublet (d); double doublet (dd); quartet (q); septet (sept) and multiplet (m).

and (H-4) at  $\delta$  4.27 ppm, were coupled once, thus showing that these groups are also terminal (Table 7). In the same spectra, we can observe three important correlations in the aromatic region. The COSY spectra show a doublet at  $\delta$  8.17 ppm ( $J = 2.0$  Hz) of (H-17), which is long-distance meta-coupled ( $^4J_{\text{H-H}}$ ) with hydrogen (H-21) at  $\delta$  7.78-7.70 ppm, which in turn, three ortho bonds ( $^3J_{\text{H-H}}$ ) are coupled ortho to hydrogen (H-21) at  $\delta$  7.78-7.70 ppm. The use of (COSY- $^3J_{\text{H-H}}$  and  $^{-4}J_{\text{H-H}}$ ) was undoubtedly a technique of great im-

portance in the attribution of the chemical displacements of hydrogens (H-3), (H-4), (H-6) and (H-14) of aliphatic and (H-17), (H-20) and (H-21) of aromatics according to Fig. (4).

According to the 2-D Heteronuclear Multiple Bond Coherence spectra (HMBC- $^2J$  and  $^{-3}J_{\text{C-H}}$ ) it was possible to unequivocally assign the couplings between  $^{13}\text{C}$  and  $^1\text{H}$  distant two and three bonds from the hydrogen coupling (H-14) of the methyl group at  $\delta$  1.13 ppm with the carbons (C-5) and (C-3) at  $\delta$  29.9 and 43.9 ppm respectively, in turn, the

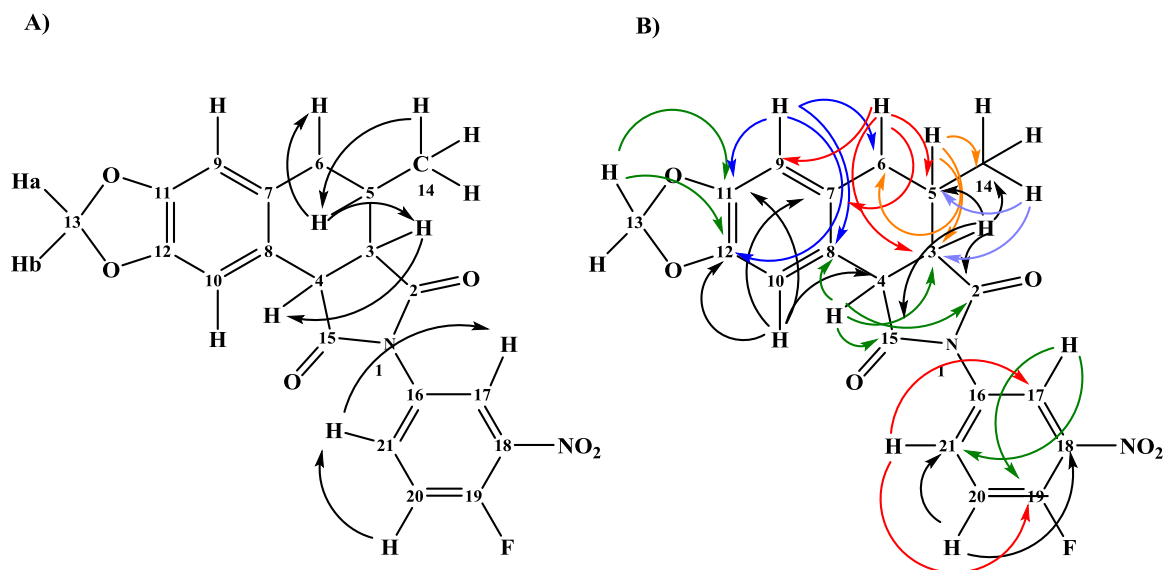


**Fig. (4).** (A) <sup>1</sup>H-<sup>1</sup>H COSY correlations of compound 5<sub>1</sub>. (B) HMBC-<sup>2</sup>J and -<sup>3</sup>J<sub>C-H</sub> correlations of compound 5<sub>1</sub>.

hydrogen (H-5) at  $\delta$  2.62 ppm next to the methyl group made two correlations with the carbons (C-6) and (C-3) at  $\delta$  34.5 and 43.9 ppm, respectively. Two important correlations were attributed to hydrogen atoms isolated from hydrogen (H-13) at  $\delta$  100.8 ppm with carbons (C-11) and (C-12) at  $\delta$  145.7 and 146.3 ppm, respectively. Other important correlations were attributed from <sup>2</sup>J and <sup>3</sup>J<sub>C-H</sub> couplings at:  $\delta$  3.52 (H-3) with 176.5 (C-2); 29.9 (C-5); 16.5 (C-14) and 175.9 (C-15) ppm;  $\delta$  4.27 (H-4) with 176.5 (C-2); 43.9 (C-3); 122.1 (C-8) and 175.9 (C-15) ppm;  $\delta$  2.26 (H-6) with 43.9 (C-3); 29.9 (C-5); 130.2 (C-7) and 108.6 (C-9) ppm. The aromatic hydrogens had their attributions confirmed from the long-distance correlations (HMBC-<sup>2</sup>J and -<sup>3</sup>J<sub>C-H</sub>) at  $\delta$  6.74 (H-9) with 34.5 (C-6); 122.1 (C-8); 145.7 (C-11) and 146.3 (C-12) ppm;  $\delta$  6.74 (H-10) with 43.4 (C-4); 130.2 (C-7); 145.7 (C-11) and 146.3 (C-12) ppm;  $\delta$  8.17 (H-17) with 153.9 (C-19) and 135.0 (C-21) ppm;  $\delta$  7.78-7.70 (H-20) with 136.7 (C-16); (C-18) and 135.0 (C-21) ppm and finally hydrogen at  $\delta$  6.74 (H-21) with 124.7 (C-17) and 153.9 (C-19) ppm (Fig. 4). The results indicated that the combined use of the one-dimensional (1-D) <sup>1</sup>H and <sup>13</sup>C-APT and two-dimensional (2-D) COSY, HETCOR and HMBC NMR techniques allowed proposing the basic skeleton of the hydrogens and carbons of 5<sub>1</sub> (Table 1) and these results were important for the assignment of signals from molecules 5<sub>2-7</sub> found in Section 2.

To verify the effectiveness of the virtual-screening method, we performed *in vitro* tests with the seven molecules synthesized (5<sub>1-7</sub>) against promastigote forms of *L. amazonensis* (IFLA/BR/1967/PH8). The results showed *pIC*<sub>50</sub> values 3.56, 3.06, 3.01, 2.98, 3.43, 3.46, 2.98, respectively. In the ligand-based approach, these seven molecules were predicted to be inactive (probabilities: 61, 53, 57, 74, 68, 63 and 65%, respectively) (Table 3), so the results of biological activity corroborate with those of *in silico* analysis, considering that our model was better at predicting inactive molecules (Table 1). It is important to highlight that this was a preliminary work, carried out to obtain candidates for drugs against *L. amazonensis* and *L. donovani*. We performed the *in vitro* tests against *L. amazonensis*, since it

was the strain available in our laboratories and the docking study for *L. donovani*, because it was the species with enzymes characterized and registered in PDB. Each study provided useful information for future works. With the material available in our laboratories we synthesized seven imides and tested them against *L. amazonensis* promastigotes and all were inactive (*pIC*<sub>50</sub> <5) as predicted in the Ligand based approach (LB). The Structure based approach (SB) for the enzymes CyP, NMT, OASS and TOPI of *L. donovani*, together with the LB, allowed the visualization of some important characteristics of the molecules that were predicted as active in our model. Molecules 5<sub>16</sub>, 5<sub>2</sub> and 5<sub>3</sub> were the most likely to be active in the LB for *L. donovani* (82, 81 and 81%, respectively). These three molecules present nitro groups in the *meta* position of the aromatic ring acting as hydrogen bonding acceptors, but without interaction pattern with specific amino acids, as can be observed in Fig. (3). Molecules 5<sub>25</sub>, 5<sub>31</sub>, 5<sub>24</sub>, 5<sub>32</sub> and 5<sub>22</sub>, with LB probabilities of activities of 75, 71, 71, 53, and 68%, respectively, are molecules which, instead of phenyl substituents, have benzylic groups substituted on the imidic nitrogen with lipophilic groups in *meta* or *para* position.

To try to rationalize the results we used Lipinski filters through the OSIRIS Property Explorer program to analyze the lipophilicity of molecules (clog P), Drug-likeness (DL) that evaluates the comparison of the investigated compounds through fragments and/or physical properties similar to those of the most known drugs, and Drug-score (DS) that combines the records of drug-likeness, lipophilicity, solubility, molecular mass and toxicity risks into a single numerical value, which varies from 0.0 to 1.0 and can be used to predict the global potential of one compound as a new drug candidate. It was observed that compounds 5<sub>16</sub>, 5<sub>2</sub> and 5<sub>3</sub>, because they have nitro groups with great toxic potential, were the compounds with lower DL and DS values (Table 6). Compound 5<sub>24</sub> which has a benzyl group with a chlorine atom substituted in *para*-position was the one with the highest values of DL and DS (Table 6).

Then, based on the findings of this study, we are proposing synthesize new molecules with benzylic substituents on imidic nitrogen with donor and acceptor of hydrogen bonds with *meta*-substituents and lipophilic groups in the *para* position. These new compounds will have great potential to act on multiple targets in parasites of the genus *Leishmania*.

## CONCLUSION

In this study, we have conducted a comparative ligand- and structure-based approach using Molegro Virtual Docking and machine learning RF to determine the anti-Leishmanial potential of thirty-three cyclic imides set. *In silico* study allowed us to suggest that the cyclic imides **5**<sub>16</sub>, **5**<sub>25</sub>, **5**<sub>31</sub>, **5**<sub>24</sub>, **5**<sub>32</sub>, **5**<sub>2</sub>, **5**<sub>3</sub> and **5**<sub>22</sub> can be tested as potential multitarget molecules for leishmanial treatment, presenting activity against four strategic enzymes for treatment with a probability of activity above 60%. So, to evaluate the efficiency of the computational method used, we have synthesized and characterized seven cyclic imides by IR, <sup>1</sup>H NMR, <sup>13</sup>C-APT NMR, COSY, HETCOR and HMBC. The compounds tested against promastigote forms of *L. amazonensis* presented *pIC*<sub>50</sub> values less than 4.7, showing that our method was efficient in predicting true negative molecules.

## ETHICS APPROVAL AND CONSENT TO PARTICIPATE

Not applicable.

## HUMAN AND ANIMAL RIGHTS

No Animals/Humans were used for studies that are base of this research.

## CONSENT FOR PUBLICATION

Not applicable.

## AVAILABILITY OF DATA AND MATERIALS

Elemental analysis for compounds 51-7, <sup>1</sup>H and <sup>13</sup>C NMR spectra for compound 51, as well as the smiles of the compounds used in the databases is available from the corresponding author, Luis JAD, upon reasonable request.

## FUNDING

This work was supported by Brazilian National Council for Scientific and Technological Development (CNPq), award Number 310919/2016-9 and 431254/2018-4.

## CONFLICT OF INTEREST

The authors declare no conflict of interest, financial or otherwise.

## ACKNOWLEDGEMENTS

Declared none.

## SUPPLEMENTARY MATERIAL

Supplementary material is available on the publisher's web site along with the published article.

## REFERENCES

- [1] Alvar, J.; Vélez, I.D.; Bern, C.; Herrero, M.; Desjeux, P.; Cano, J.; Jannin, J.; den Boer, M.; Team, W.L.C. WHO leishmaniasis control team. Leishmaniasis worldwide and global estimates of its incidence. *PLoS One*, **2012**, *7*(5), e35671. [http://dx.doi.org/10.1371/journal.pone.0035671] [PMID: 22693548]
- [2] Rodrigues, K.A.F.; Dias, C.N.S.; Nérís, P.L.N.; Rocha, J.C.; Scotti, M.T.; Scotti, L.; Mascarenhas, S.R.; Veras, R.C.; de Medeiros, I.A.; Keesen, Tde.S.; de Oliveira, T.B.; de Lima, M.C.; Balliano, T.L.; de Aquino, T.M.; de Moura, R.O.; Mendonça Junior, F.J.; de Oliveira, M.R. 2-Amino-thiophene derivatives present antileishmanial activity mediated by apoptosis and immunomodulation *in vitro*. *Eur. J. Med. Chem.*, **2015**, *106*, 1-14. [http://dx.doi.org/10.1016/j.ejmech.2015.10.011] [PMID: 26513640]
- [3] Bonano, V.I.; Yokoyama-Yasunaka, J.K.; Miguel, D.C.; Jones, S.A.; Dodge, J.A.; Uliana, S.R. Discovery of synthetic Leishmania inhibitors by screening of a 2-arylbenzothiofene library. *Chem. Biol. Drug Des.*, **2014**, *83*(3), 289-296. [http://dx.doi.org/10.1111/cbdd.12239] [PMID: 24119198]
- [4] Herrera Acevedo, C.; Scotti, L.; Feitosa Alves, M.; Formiga Melo Diniz, M.F.; Scotti, M.T. Computer-aided drug design using sesquiterpene lactones as sources of new structures with potential activity against infectious neglected diseases. *Molecules*, **2017**, *22*(1), 79. [http://dx.doi.org/10.3390/molecules22010079] [PMID: 28054952]
- [5] Thompson, A.M.; O'Connor, P.D.; Marshall, A.J.; Yardley, V.; Maes, L.; Gupta, S.; Launay, D.; Braillard, S.; Chatelain, E.; Franzblau, S.G.; Wan, B.; Wang, Y.; Ma, Z.; Cooper, C.B.; Denny, W.A. 7-substituted 2-nitro-5,6-dihydroimidazo[2,1-b][1,3]oxazines: Novel antitubercular agents lead to a new preclinical candidate for visceral leishmaniasis. *J. Med. Chem.*, **2017**, *60*(10), 4212-4233. [http://dx.doi.org/10.1021/acs.jmedchem.7b00034] [PMID: 28459575]
- [6] Ogungbe, I.V.; Erwin, W.R.; Setzer, W.N. Antileishmanial phytochemical phenolics: molecular docking to potential protein targets. *J. Mol. Graph. Model.*, **2014**, *48*, 105-117. [http://dx.doi.org/10.1016/j.jmgm.2013.12.010] [PMID: 24463105]
- [7] Hermoso, A.; Jiménez, I.A.; Mamani, Z.A.; Bazzocchi, I.L.; Piñero, J.E.; Ravelo, A.G.; Valladares, B. Antileishmanial activities of dihydrochalcones from piper elongatum and synthetic related compounds. Structural requirements for activity. *Bioorg. Med. Chem.*, **2003**, *11*(18), 3975-3980. [http://dx.doi.org/10.1016/S0968-0896(03)00406-1] [PMID: 12927858]
- [8] Lill, M.A.; Danielson, M.L. Computer-aided drug design platform using PyMOL. *J. Comput. Aided Mol. Des.*, **2011**, *25*(1), 13-19. [http://dx.doi.org/10.1007/s10822-010-9395-8] [PMID: 21053052]
- [9] Lorenzo, V.P.; Lúcio, A.S.; Scotti, L.; Tavares, J.F.; Filho, J.M.; Lima, T.K.; Rocha, J.D.; Scotti, M.T. Structure- and ligand-based approaches to evaluate aporphinic alkaloids from annonaceae as multi-target agent against Leishmania donovani. *Curr. Pharm. Des.*, **2016**, *22*(34), 5196-5203. [http://dx.doi.org/10.2174/1381612822666160513144853] [PMID: 27174814]
- [10] Lorenzo, V.P.; Barbosa-Filho, J.M.; Scotti, L.; Scotti, M.T. Combined structure- and ligand-based virtual screening to evaluate caulerpin analogs with potential inhibitory activity against monoamine oxidase B. *Rev. Bras. Farmacogn.*, **2015**, *25*(6), 690-697. [http://dx.doi.org/10.1016/j.bjpp.2015.08.005]
- [11] Hargreaves, M.K.; Pritchard, J.; Dave, H. Cyclic carboxylic monoimides. *Chem. Rev.*, **1970**, *70*(4), 439-469. [http://dx.doi.org/10.1021/cr60266a001]
- [12] Cechinel-Filho, V. Principais avanços e perspectivas na área de produtos naturais ativos: estudos desenvolvidos no NIOFAR/UNIVALI. *Quim. Nova*, **2000**, *23*(5), 680-685. [http://dx.doi.org/10.1590/S0100-40422000000500017]
- [13] Cechinel Filho, V.; Pinheiro, T.; Nunes, R.J.; Yunes, R.A.; Cruz, A.B.; Moretto, E. Antibacterial activity of N-phenylmaleimides, N-phenylsuccinimides and related compounds. Structure-activity relationships. *Farmaco*, **1994**, *49*(10), 675-677. [PMID: 7826477]

- [14] Yunes, J.A.; Cardoso, A.A.; Yunes, R.A.; Correa, R.; de Campos-Buzzi, F.; Cechinel-Filho, V.Z. Antiproliferative effects of a series of cyclic imides on primary endothelial cells and a leukemia cell line. *Naturforsch. C*, **2008**, *63*(9-10), 675-680. [http://dx.doi.org/10.1515/znc-2008-9-1011] [PMID: 19040106]
- [15] Zawadowski, T.; Kossakowski, J.; Rump, S.; Jakowicz, I.; Płażnik, A. Synthesis and anxiolytic activity of N-substituted cyclic imides N-[4-[(4-aryl)-1-piperazinyl]alkyl]-5,7-dioxabicyclo[2.2.2]octane-2, 3-dicarboximide. *Acta Pol. Pharm.*, **1995**, *52*(1), 43-46. [PMID: 8960237]
- [16] Alaa, A-M. Novel and versatile methodology for synthesis of cyclic imides and evaluation of their cytotoxic, DNA binding, apoptotic inducing activities and molecular modeling study. *Eur. J. Med. Chem.*, **2007**, *42*(5), 614-626. [http://dx.doi.org/10.1016/j.ejmech.2006.12.003] [PMID: 17234303]
- [17] Mesomo, M.C.; Corazza, M.L.; Ndiaye, P.M.; Dalla Santa, O.R.; Cardozo, L.; Scheer, A.R.P. Supercritical CO<sub>2</sub> extracts and essential oil of ginger (*Zingiber officinale* R.): Chemical composition and antibacterial activity. *J. Supercrit. Fluids*, **2013**, *80*, 44-49. [http://dx.doi.org/10.1016/j.supflu.2013.03.031]
- [18] Povh, N.P.; Marques, M.O.; Meireles, M.A.A. Supercritical CO<sub>2</sub> extraction of essential oil and oleoresin from chamomile (*Chamomilla recutita* [L.] Rauschert). *J. Supercrit. Fluids*, **2001**, *21*(3), 245-256. [http://dx.doi.org/10.1016/S0896-8446(01)00096-1]
- [19] Imre, G.; Veress, G.; Volford, A.; Farkas, Ö. Molecules from the Minkowski space: an approach to building 3D molecular structures. *J. Mol. Struct. THEOCHEM*, **2003**, *666*, 51-59. [http://dx.doi.org/10.1016/j.theochem.2003.08.013]
- [20] Cruciani, G.; Crivori, P.; Carrupt, P-A.; Testa, B. Molecular fields in quantitative structure-permeation relationships: the VolSurf approach. *J. Mol. Struct. THEOCHEM*, **2000**, *503*(1), 17-30. [http://dx.doi.org/10.1016/S0166-1280(99)00360-7]
- [21] Scotti, L.; Ishiki, H.; Mendonça Júnior, F.J.; Da Silva, M.S.; Scotti, M.T. *In-silico* analyses of natural products on leishmania enzyme targets. *Mini Rev. Med. Chem.*, **2015**, *15*(3), 253-269. [http://dx.doi.org/10.2174/138955751503150312141854] [PMID: 25769973]
- [22] Scotti, L.; Scotti, M.T. Computer aided drug design studies in the discovery of secondary metabolites targeted against age-related neurodegenerative diseases. *Curr. Top. Med. Chem.*, **2015**, *15*(21), 2239-2252. [http://dx.doi.org/10.2174/1568026615666150610143510] [PMID: 26059353]
- [23] Berthold, M.R.C.N.; Dill, F. *Data analysis, machine learning and applications*. Springer: Berlin, **2007**; pp. 36-79.
- [24] Breiman, L. Random forests. *Mach. Learn.*, **2001**, *45*(1), 5-32. [http://dx.doi.org/10.1023/A:1010933404324]
- [25] Hall, M.; Frank, E.; Holmes, G.; Pfahringer, B.; Reutemann, P.; Witten, I.H. The WEKA data mining software: an update. *Explorations newsletter*, **2009**, *11*(1), 10-18. [https://doi.org/10.1145/1656274.1656278]
- [26] Hanley, J.A.; McNeil, B.J. The meaning and use of the area under a receiver operating characteristic (ROC) curve. *Radiology*, **1982**, *143*(1), 29-36. [http://dx.doi.org/10.1148/radiology.143.1.7063747] [PMID: 7063747]
- [27] Davies, D.R.; Mushtaq, A.; Interthal, H.; Champoux, J.J.; Hol, W.G. The structure of the transition state of the heterodimeric topoisomerase I of *Leishmania donovani* as a vanadate complex with nicked DNA. *J. Mol. Biol.*, **2006**, *357*(4), 1202-1210. [http://dx.doi.org/10.1016/j.jmb.2006.01.022] [PMID: 16487540]
- [28] Rackham, M.D.; Yu, Z.; Brannigan, J.A.; Heal, W.P.; Paape, D.; Barker, K.V.; Wilkinson, A.J.; Smith, D.F.; Leatherbarrow, R.J.; Tate, E.W. Discovery of high affinity inhibitors of *Leishmania donovani* N-myristoyltransferase. *MedChemComm*, **2015**, *6*(10), 1761-1766. [http://dx.doi.org/10.1039/C5MD00241A] [PMID: 26962429]
- [29] Venugopal, V.; Datta, A.K.; Bhattacharyya, D.; Dasgupta, D.; Banerjee, R. Structure of cyclophilin from *Leishmania donovani* bound to cyclosporin at 2.6 Å resolution: correlation between structure and thermodynamic data. *Acta Crystallogr. D Biol. Crystallogr.*, **2009**, *65*(Pt 11), 1187-1195. [http://dx.doi.org/10.1107/S0907444909034234] [PMID: 19923714]
- [30] Raj, I.; Kumar, S.; Gourinath, S. The narrow active-site cleft of O-acetylserine sulfhydrylase from *Leishmania donovani* allows complex formation with serine acetyltransferases with a range of C-terminal sequences. *Acta Crystallogr. D Biol. Crystallogr.*, **2012**, *68*(Pt 8), 909-919. [http://dx.doi.org/10.1107/S0907444912016459] [PMID: 22868756]
- [31] Thomsen, R.; Christensen, M.H. MolDock: a new technique for high-accuracy molecular docking. *J. Med. Chem.*, **2006**, *49*(11), 3315-3321. [http://dx.doi.org/10.1021/jm051197e] [PMID: 16722650]
- [32] Hudson, B.; Robinson, R. Addition of maleic anhydride and ethyl maleate to substituted styrenes. *J. Chem. Soc.*, **1941**, 715-722. [http://dx.doi.org/10.1039/jr9410000715]
- [33] García, I.; Fall, Y.; Gómez, G.; González-Díaz, H. First computational chemistry multi-target model for anti-Alzheimer, anti-parasitic, anti-fungi, and anti-bacterial activity of GSK-3 inhibitors *in vitro*, *in vivo*, and in different cellular lines. *Mol. Divers.*, **2011**, *15*(2), 561-567. [http://dx.doi.org/10.1007/s11030-010-9280-3] [PMID: 20931280]
- [34] Barreiro, E.J.; Lima, M.E. The synthesis and anti-inflammatory properties of a new sulindac analogue synthesized from natural safrole. *J. Pharm. Sci.*, **1992**, *81*(12), 1219-1222. [http://dx.doi.org/10.1002/jps.2600811219] [PMID: 1491344]